symmetry

MDPI

Article

Robustness of Consensus of Two-Layer Ring Networks

Zhijun Li [1], Haiping Gao [2], Zhiyong Shang [3,*] and Wenming Zhang [4]

[1] Academic Affairs Office, Xinjiang Institute of Light Industry Technology, Urumqi 830023, China
[2] Department of Basic Science, Xinjiang Institute of Light Industry Technology, Urumqi 830023, China
[3] Mechanical Engineering Laboratory, Xinjiang Institute of Engineering, Urumqi 830023, China
[4] Department of Information and Software, Xinjiang Institute of Light Industry Technology, Urumqi 830023, China
* Correspondence: szy@xjie.edu.cn

Abstract: The topology structure of multi-layer networks is highly correlated with the robustness of consensus. This paper investigates the influence of different interlayer edge connection patterns on the consensus of the two-layer ring networks. Two types of two-layer ring network models are first considered: one is a kind of two-layer ring network with two linked edges between layers (Networks-a), and the other is a kind of two-layer ring network with three linked edges between layers (Networks-b). Using the Laplacian spectrum, the consensus of the network model is derived. The simulation experiments are used to demonstrate the influence of different interlayer edge connection patterns on the consensus of networks. To determine the best edge connection pattern for Networks-a and Networks-b, the number of nodes in a single-layer ring network is denoted by n. The best edge connection pattern for Networks-a is 1 & $[(n+2)/2]$. Furthermore, n is subdivided into $3k, 3k+1, 3k+2$, and the best edge connection patterns of Networks-b are near 1 & $k+1$ & $2k+1$.

Keywords: multi-layer ring network; topology structure; consensus; robustness; edge connection patterns

Citation: Li, Z.; Gao, H.; Shang, Z.; Zhang, W. Robustness of Consensus of Two-Layer Ring Networks. *Symmetry* **2023**, *15*, 1085. https://doi.org/10.3390/sym15051085

Academic Editors: Chong Wang and Alexander Zaslavski

Received: 1 March 2023
Revised: 4 May 2023
Accepted: 9 May 2023
Published: 15 May 2023

1. Introduction

Complex networks have been widely used in fields such as earth sciences, robot control, biological systems, and neuroscience [1–5]. With the deepening of the research, scholars have found that most complex systems are not isolated, but are instead interdependent and interactive. Researchers introduced the concept of multi-layer networks to describe such networks and have made fruitful achievements in the field of research on multi-layer networks, such as accomplishing the synchronization of multi-layer complex networks [6–12], structure identification of multi-layer networks [13], and cascading failures and consensus of multi-layer networks [14–18].

Noise exists in the real environment. Not all nodes of the complex network may achieve the common goal well under the interference of noise. Network coherence is used to study the degree of consensus that can be achieved by all nodes of the network and describes the deviation of the state of each node in the network from the average of the current states of all nodes. Network coherence is determined by the Laplacian spectrum [19]. Ref. [20] discussed the robustness of a scale-free network consensus and discovered the relationships between network coherence and average degree. Ref. [21] calculated the Laplacian eigenvalues of a class of fractal networks using a recursive method and obtained the first-order and second-order coherence of the networks. Ref. [22] designed a new control protocol to study the consensus of multi-intelligent systems. Ref. [23] presented an algorithm for approximating second-order coherence. Ref. [24] studied the robustness of network coherence and found that asymmetric networks show higher coherence than symmetric networks. The above literature has mainly studied the impact of control protocol design and topology on network consensus but has not considered the impact of different layer connection methods on network consensus.

As the basic elements of the network, the ring structure, link structure, and star structure play a very important role in the complex network. Unlike the link and star structure, the ring structure brings redundant paths to its nodes, which greatly enhances the connectivity of the network and becomes more robust. Research on the ring structure can provide new ideas and methods for optimizing network connectivity and anti-attack capability, quickly adjusting the network state. Therefore, a network based on a ring structure has aroused great interest in scholars and has achieved some good results [25–27].

Consensus-based distributed algorithms have been widely studied in the field of networked systems for achieving agreement among a group of agents with limited communication abilities [28,29]. A large-scale, many-objective deployment optimization algorithm for edge servers in a networked system was proposed, which is relevant to the consensus problem [28]. In a consensus problem, agents aim to reach a common decision based on local interactions with their neighbors, which can be modeled as a network. One of the most widely used network structures for consensus is the two-layer ring network, which is robust and efficient at achieving agreement among a group of agents. However, the robustness of consensus in these networks is still an open research question [30,31]. A robust identification method for highly nonlinear systems was proposed, which is important for achieving consensus in the presence of noise and disturbances [30]. This paper takes the two-layer ring networks as the research object and analyzes the influence of different interlayer edge-connection patterns on the consensus of the two-layer ring networks. The main novelties and contributions of the paper are as follows:

1. A new network model is proposed that is different from the interlayer, fully connected two-layer ring networks. This will save more costs in practical applications.
2. Compared with solving the Laplacian spectrum of the fully connected network, the Laplacian spectrum of the partially connected two-layer ring networks is difficult to calculate. The consensus of the two-layer ring networks is obtained by using the relationships among the network coherence, eigenvalues, and characteristic polynomial coefficients.
3. Based on the formula of network coherence, the optimal and worst edge-connected patterns of two-layer ring networks are found, and the results are revealed through simulation experiments.

The paper is organized as follows. The preliminaries are given in Section 2. The consensus is derived in Section 3. Section 4 presents the numerical simulation results.

2. Preliminaries

2.1. Network Coherence

The research on consensus not only helps to better understand the general mechanism of consensus in nature but also helps to reveal the essence of some practical engineering operations, such as the coordination and control of distributed sensors and the control of multi-robot formations.

The network dynamics model with q nodes is described as follows [32]:

$$\dot{x}(t) = -Lx(t) + \varepsilon(t), \tag{1}$$

where $L \in R^{q\times q}$ is the Laplacian matrix of the network and $\varepsilon(t) \in R^q$ represents the interference of white noise. Network coherence is defined as robustness to noise:

$$H^1 = \frac{1}{q}\sum_{i=1}^{q}\lim_{t\to\infty}\mathrm{var}\left(x_i(t) - \frac{1}{q}\sum_{j=1}^{q}x_j(t)\right). \tag{2}$$

The output of system (1) is written as follows:

$$y = Px, \tag{3}$$

where P is the projection operator, $P = I - \frac{1}{q}\mathbf{1}\mathbf{1}^{T}$ and $\mathbf{1}$ is the q-vector of all ones.

Using Formula (1)–(3),

$$H^{1} = \frac{1}{q}\mathrm{tr}\left(\int_{0}^{\infty} e^{-L^{T}t} P e^{-Lt} dt\right). \tag{4}$$

According to [33], the first-order coherence can be expressed in terms of Laplacian eigenvalues,

$$H^{1} = \frac{1}{2q}\sum_{\nu=2}^{q}\frac{1}{\lambda_{\nu}}. \tag{5}$$

2.2. Two-Layer Ring Network Models

A kind of two-layer ring network with two linked edges between layers (Networks-a) is shown in Figure 1a. Due to the symmetry of the ring network, we assume that there are two edges between node pairs 1 and $p(2 \le p \le n)$, where n is the number of nodes in the ring network. We denote the edge connection pattern as $1\ \&p$. A kind of two-layer ring network with three linked edges between layers (Networks-b) is shown in Figure 1b. We assume that there are three edges between node pairs 1, $i(2 \le i \le n-1)$, and $j(i+1 \le j \le n)$, and we denote the edge connection pattern as $1\ \&\ i\ \&\ j$.

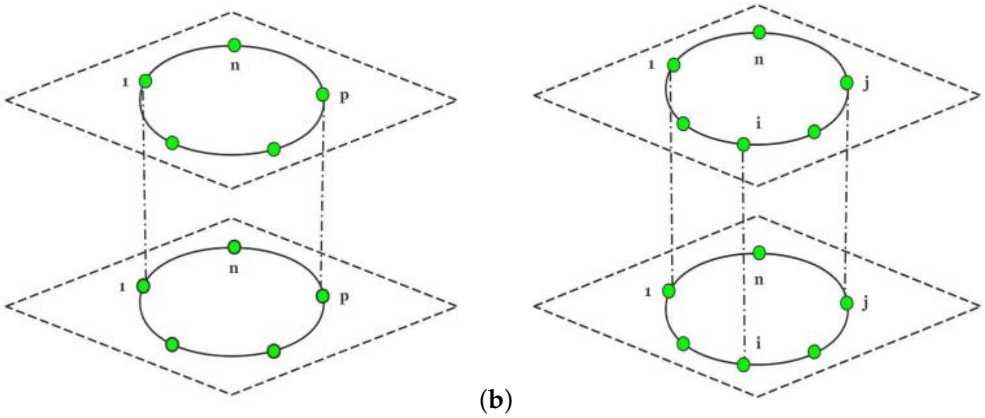

(**a**) (**b**)

Figure 1. (**a**) Schematic diagram of Networks-a. (**b**) Schematic diagram of Networks-b.

3. Theoretical Calculation and Conjectures

In this section, we calculate the coherence of Networks-a and Networks-b and make some conjectures about the influence of different edge connection patterns on the consensus.

3.1. The Coherence H^{1a} of Networks-a

This section will use the relationships between the eigenvalues and coefficients in characteristic polynomial theory to obtain the coherence of Networks-a. To solve this problem, the coefficients of a class of characteristic polynomials are as follows:

Lemma 1 ([20]). *Let $R_n(0), R_n(1), R_n(2)$ be the constant term, first-order coefficient and quadratic coefficient of the characteristic polynomial $R_n(\lambda)$,*

$$R_n(\lambda) = \begin{vmatrix} \lambda-2 & 1 & & & & & \\ 1 & \lambda-2 & 1 & & & & \\ & 1 & \lambda-2 & 1 & & & \\ & & 1 & \lambda-2 & & & \\ & & & & \ddots & & \\ & & & & & \lambda-2 & 1 \\ & & & & & 1 & \lambda-2 \end{vmatrix}_{n\times n},$$

then, $R_n(0) = (-1)^n(n+1)$, $R_n(1) = (-1)^{n-1}\frac{n(n+1)(n+2)}{6}$, $R_n(2) = (-1)^{n-2}\frac{(n-1)n(n+1)(n+2)(n+3)}{120}$.

According to the topology structure of Networks-a, the Laplacian characteristic polynomial is $|\lambda I_n - A_1 - B_1||\lambda I_n - A_1 + B_1|$.

$$|\lambda I_n - A_1 - B_1| = \begin{vmatrix} \lambda-2 & 1 & 0 & 0 & \cdots & 0 & 1 \\ 1 & \lambda-2 & 1 & 0 & \cdots & 0 & 0 \\ 0 & 1 & \lambda-2 & 1 & \cdots & 0 & 0 \\ 0 & 0 & 1 & \lambda-2 & \cdots & 0 & 0 \\ \vdots & \vdots & \vdots & \vdots & \ddots & \vdots & \vdots \\ 0 & 0 & 0 & 0 & \cdots & \lambda-2 & 1 \\ 1 & 0 & 0 & 0 & \cdots & 1 & \lambda-2 \end{vmatrix}_{n\times n},$$

$$|\lambda I_n - A_1 + B_1| = \begin{vmatrix} \lambda-4 & 1 & 0 & \cdots & 0 & 0 & \cdots & 1 \\ 1 & \lambda-2 & 1 & \cdots & 0 & 0 & \cdots & 0 \\ 0 & 1 & \lambda-2 & \cdots & 0 & 0 & \cdots & 0 \\ \vdots & \vdots & \vdots & \ddots & \vdots & \vdots & & \vdots \\ 0 & 0 & 0 & \cdots & \lambda-4 & 1 & \cdots & 0 \\ 0 & 0 & 0 & \cdots & 1 & \lambda-2 & \cdots & 0 \\ \vdots & \vdots & \vdots & & \vdots & \vdots & \ddots & \vdots \\ 1 & 0 & 0 & \cdots & 0 & 0 & \cdots & \lambda-2 \end{vmatrix}_{n\times n}.$$

Let $|\lambda I_n - A_1 - B_1|$ *be* $C_n(\lambda)$; $C_n(\lambda)$ *is the Laplacian characteristic polynomial of the ring network* C_n. *We expand* $|\lambda I_n - A_1 - B_1|$ *using the first row,*

$$C_n(\lambda) = (\lambda-2)R_{n-1}(\lambda) - 2R_{n-2}(\lambda) + 2(-1)^{n+1}. \tag{6}$$

$|\lambda I_n - A_1 + B_1|$ *can be obtained by changing the 1st and pth diagonal elements to* $\lambda - 4$ *on the basis of* $|\lambda I_n - A_1 - B_1|$. *Let* $|\lambda I_n - A_1 + B_1|$ *be* $S_n(\lambda)$; *combining the relationships between* $S_n(\lambda)$ *and* $C_n(\lambda)$, *we have*

$$\begin{aligned} S_n(\lambda) =& C_n(\lambda) - 2R_{p-1}(\lambda)R_{n-p}(\lambda) + 2R_{p-2}(\lambda)R_{n-p-1}(\lambda) \\ & - 2R_{n-1}(\lambda) + 4R_{p-2}(\lambda)R_{n-p}(\lambda). \end{aligned} \tag{7}$$

We will use Lemma 1 to obtain the sum of the reciprocals of the non-zero characteristic eigenvalues of $C_n(\lambda)$ *and* $S_n(\lambda)$, *respectively. For the convenience of description, let* $C_m(i)$, $S_m(i)$, $R_m(i)$ $(i = 0, 1, 2)$ *be the i degree coefficients of* $C_m(\lambda)$, $S_m(\lambda)$, $R_m(\lambda)$, *respectively.*

Lemma 2. *Let* $0 = \gamma_1 < \gamma_2 \leq \cdots \leq \gamma_n$ *be the eigenvalues of* $C_n(\lambda)$; *then,*

$$\sum_{l=2}^{n} \frac{1}{\gamma_l} = \frac{n^2-1}{12}.$$

Proof. From the Vieta theorem [21], $\sum_{l=2}^{n} \frac{1}{\gamma_l} = -\frac{C_n(2)}{C_n(1)}$, using Lemma 1,

$$\begin{aligned} \sum_{l=2}^{n} \frac{1}{\gamma_l} &= -\frac{R_{n-1}(1) - 2R_{n-1}(2) - 2R_{n-2}(2)}{R_{n-1}(0) - 2R_{n-1}(1) - 2R_{n-2}(1)} \\ &= \frac{(-1)^{n-1}\frac{(n-1)n(n+1)}{6} + (-1)^{n-1}\frac{(n-2)(n-1)n(n+1)}{12}}{(-1)^{n-1}n - (-1)^{n-2}\frac{(n-1)n(n+1)}{3} - (-1)^{n-3}\frac{(n-2)(n-1)n}{3}} \\ &= \frac{n^2-1}{12}. \end{aligned} \tag{8}$$

□

Lemma 3. *Let* $0 < \kappa_1 \leq \kappa_2 \leq \cdots \leq \kappa_n$ *be the eigenvalues of* $S_n(\lambda)$*; then,*

$$\sum_{r=1}^{n} \frac{1}{\kappa_r} = \frac{n^3 + 3n^2 - n + (p-1)p(2np - 2p^2 + 4p - n - 3)}{12n + 12(p-1)(n-p+1)} + \frac{(n-p)(n-p+1)(2np - 2p^2 + 8p - n - 5)}{12n + 12(p-1)(n-p+1)}.$$

Proof. From the Vieta theorem, $\sum_{r=1}^{n} \frac{1}{\kappa_r} = -\frac{S_n(1)}{S_n(0)}$, using Lemma 1,

$$\sum_{r=1}^{n} \frac{1}{\kappa_r} = -\frac{C_n(1) - 2f_1(0,1) + 2f_2(0,1) - 2R_{n-1}(1) + 4f_3(0,1)}{-2R_{p-1}(0)R_{n-p}(0) + 2R_{p-2}(0)R_{n-p-1}(0) - 2R_{n-1}(0) + 4R_{p-2}(0)R_{n-p}(0)},$$

where

$$\begin{aligned}
f_1(0,1) &= R_{p-1}(1)R_{n-p}(0) + R_{p-1}(0)R_{n-p}(1) \\
&= (-1)^{n-2}\frac{p(n-p+1)}{6}[(p-1)(p+1) + (n-p)(n-p+2)], \\
f_2(0,1) &= R_{p-2}(1)R_{n-p-1}(0) + R_{p-2}(0)R_{n-p-1}(1) \\
&= (-1)^{n-4}\frac{(p-1)(n-p)}{6}[(p-2)p + (n-p-1)(n-p+1)], \\
f_3(0,1) &= R_{p-2}(1)R_{n-p}(0) + R_{p-2}(0)R_{n-p}(1) \\
&= (-1)^{n-3}\frac{(p-1)(n-p+1)}{6}[(p-2)p + (n-p)(n-p+2)], \\
R_{p-1}(0)R_{n-p}(0) &= (-1)^{n-1}p(n-p+1), \\
R_{p-2}(0)R_{n-p-1}(0) &= (-1)^{n-3}(p-1)(n-p), \\
R_{p-2}(0)R_{n-p}(0) &= (-1)^{n-2}(p-1)(n-p+1),
\end{aligned}$$

then

$$\sum_{r=1}^{n} \frac{1}{\kappa_r} = \frac{n^3 + 3n^2 - n + (p-1)p(2np - 2p^2 + 4p - n - 3)}{12n + 12(p-1)(n-p+1)} + \frac{(n-p)(n-p+1)(2np - 2p^2 + 8p - n - 5)}{12n + 12(p-1)(n-p+1)}. \tag{9}$$

□

Theorem 1. *Let the number of single-layer network nodes in Networks-a be n. If there are two linked edges between the node pairs 1 and* $p(2 \leq p \leq n)$*, then the coherence* H^{1a} *of Networks-a is as follows:*

$$H^{1a} = \frac{1}{4n}\left[\frac{n^2-1}{12} + \frac{n^3 + 3n^2 - n + (p-1)p(2np - 2p^2 + 4p - n - 3)}{12n + 12(p-1)(n-p+1)} + \frac{(n-p)(n-p+1)(2np - 2p^2 + 8p - n - 5)}{12n + 12(p-1)(n-p+1)}\right].$$

Proof. Using Formula (5),

$$H^{1a} = \frac{1}{4n}\left[\sum_{l=2}^{n} \frac{1}{\gamma_l} + \sum_{r=1}^{n} \frac{1}{\kappa_r}\right] \tag{10}$$

By substituting the results of Equations (8) and (9) into Equation (10), Theorem 1 can be easily obtained. □

3.2. The Coherence H^{1b} of Networks-b

Similar to Section 3.1, this section will use the coefficients of the characteristic polynomial to obtain the coherence of Networks-b.

According to the topology of Networks-b, the Laplacian characteristic polynomial can be written as follows:

$$\begin{vmatrix} \lambda I_n - A_2 & -B_2 \\ -B_2 & \lambda I_n - A_2 \end{vmatrix} = |\lambda I_n - A_2 - B_2||\lambda I_n - A_2 + B_2|.$$

$$|\lambda I_n - A_2 + B_2| = \begin{vmatrix} \lambda-4 & 1 & \cdots & 0 & 0 & \cdots & 0 & 0 & \cdots & 1 \\ 1 & \lambda-2 & \cdots & 0 & 0 & \cdots & 0 & 0 & \cdots & 0 \\ \vdots & \vdots & \ddots & \vdots & \vdots & & \vdots & \vdots & & \vdots \\ 0 & 0 & \cdots & \lambda-4 & 1 & \cdots & 0 & 0 & \cdots & 0 \\ 0 & 0 & \cdots & 1 & \lambda-2 & \cdots & 0 & 0 & \cdots & 0 \\ \vdots & \vdots & & \vdots & \vdots & \ddots & \vdots & \vdots & & \vdots \\ 0 & 0 & \cdots & 0 & 0 & \cdots & \lambda-4 & 1 & \cdots & 0 \\ 0 & 0 & \cdots & 0 & 0 & \cdots & 1 & \lambda-2 & \cdots & 0 \\ \vdots & \vdots & & \vdots & \vdots & & \vdots & \vdots & \ddots & \vdots \\ 1 & 0 & \cdots & 0 & 0 & \cdots & 0 & 0 & \cdots & \lambda-2 \end{vmatrix}_{n\times n}.$$

$|\lambda I_n - A_2 + B_2|$ can be obtained by changing the 1st, ith, and jth diagonal elements to $\lambda - 4$ on the basis of $|\lambda I_n - A_2 - B_2|$. Let $|\lambda I_n - A_2 + B_2|$ be $Q_n(\lambda)$; using the Laplacian theorem, we get $Q_n(\lambda) = C_n(\lambda) - 2R_{n-1}(\lambda) - 2R_{i-1}(\lambda)R_{n-i}(\lambda) + 2R_{i-2}(\lambda)(R_{n-i-1}(\lambda) + 2R_{n-i}(\lambda)) - 2R_{j-1}(\lambda)R_{n-j}(\lambda) + 2R_{j-2}(\lambda)(R_{n-j-1}(\lambda) + 2R_{n-j}(\lambda)) + 4R_{j-i-1}(\lambda)(R_{i-1}(\lambda) R_{n-j}(\lambda) - R_{i-2}(\lambda)R_{n-j-1}(\lambda) - 2R_{i-2}(\lambda)R_{n-j}(\lambda))$.

Theorem 2. *Let the number of single-layer network nodes in Networks-b be n. If there are three linked edges between the node pairs 1, $i(2 \le i \le n-1)$, and $j(i+1 \le j \le n)$, then the coherence H^{1b} of Networks-b is as follows:*

$$H^{1b} = \frac{1}{4n}\left[\frac{n^2-1}{12} + \frac{f_1(n,i,j)}{f_2(n,i,j)}\right],$$

where $f_1(n,i,j) = n^3 + 3n^2 - n + (j-1)j(2nj - 2j^2 + 4j - n - 3) + (n-j)(n-j+1)(2nj - 2j^2 + 8j - n - 5) + (i-1)i(2ni - 2i^2 + 4i - n - 3) + (n-i)(n-i+1)(2ni - 2i^2 + 8i - n - 5) + 2(i-1)i(j-i)(2ni - 2ij + 3i + j - n - 3) + 2(j-i-1)(j-i)(j-i+1)(2ni - 2ij + 3i + j - n - 2) + 2(j-i)(n-j)(n-j+1)(2ni - 2ij + 7i + j - n - 5)$,

$f_2(n,i,j) = 48i - 6n + 24ij + 24ni - 24ij^2 + 24i^2j - 24i^2n - 48i^2 + 24ijn - 24$.

Proof. Let $0 = \nu_1 < \nu_2 \le \cdots \le \nu_n$ be the eigenvalues of $Q_n(\lambda)$; using the Formula (5),

$$H^{1b} = \frac{1}{4n}\left[\sum_{l=2}^{n}\frac{1}{\gamma_l} + \sum_{q=1}^{n}\frac{1}{\nu_q}\right]. \tag{11}$$

Similar to the proof of Lemma 3, we have $\sum_{q=1}^{n}\frac{1}{\nu_q} = \frac{f_1(n,i,j)}{f_2(n,i,j)}$. Theorem 2 can be easily obtained. □

3.3. Conjecture

Conjecture 1. *The impact of edge connection pattern 1 & p on the consensus of Networks-a is as follows:*

(1) When n is odd, the edge connection patterns 1 & $(n+1)/2$ and 1 & $(n+3)/2$ have the best network consensus.
(2) When n is even, the edge connection pattern 1 & $(n+2)/2$ has the best network consensus.
(3) Whether n is odd or even, the edge connection patterns 1 & 2 and 1 & n have the worst network consensus.

Conjecture 2. *The impact of edge connection pattern 1 & i & j on the consensus of Networks-b is as follows:*

(1) *The edge connection patterns 1 & 2 & 3, 1 & 2 & n, and 1 & $n-1$ & n have the worst network consensus.*
(2) *When i is fixed, $i+1 \leq j \leq n$, and the edge connection patterns 1 & i & $i+1$ and 1 & i & n have the worst network consensus. When $n+i+1$ is odd, the edge connection patterns 1 & i & $(n+i)/2$ and 1 & i & $(n+i+2)/2$ have the best network consensus. When $n+i+1$ is even, the edge connection pattern 1 & i & $(n+i+1)/2$ has the best network consensus.*

Conjecture 3. *The impact of the number of single-layer network nodes n on the consensus of Networks-b is as follows:*

When $n = 3k$, the edge connection pattern 1 & $k+1$ & $2k+1$ has the best network consensus. When $n = 3k+1$, the edge connection patterns 1 & $k+1$ & $2k+1$, 1 & $k+1$ & $2k+2$, and 1 & $k+2$ & $2k+2$ have the best network consensus. When $n = 3k+2$, the edge connection patterns 1 & $k+1$ & $2k+2$, 1 & $k+2$ & $2k+2$, and 1 & $k+2$ & $2k+3$ have the best network consensus.

4. Numerical Simulation Experiment

In this section, the relationships between the edge connection patterns and consensus are numerically simulated to demonstrate the rationality of the three conjectures mentioned in the previous section.

4.1. The Influence of Edge Connection Pattern 1 & p on H^{1a}

When $n = 15, 20, 25, 30, 35$, through the traversal simulation of all edge connection patterns 1 & p, Figure 2 shows the change in H^{1a} with p. When $2 \leq p \leq (n+2)/2$, H^{1a} decreases with the increase in p. When $(n+2)/2 < p \leq n$, H^{1a} increases with the increase in p. As p can only be a positive integer, H^{1a} obtains the maximum value at $p = 2$ and $p = n$ and obtains the minimum value at $p = [(n+2)/2]$. The smaller the first-order coherence is, the stronger the consensus is. The edge connection pattern 1 & $[(n+2)/2]$ has the best consensus, and the edge connection patterns 1 & 2 and 1 & n have the worst network consensus; this result is consistent with the conclusion of Conjecture 1.

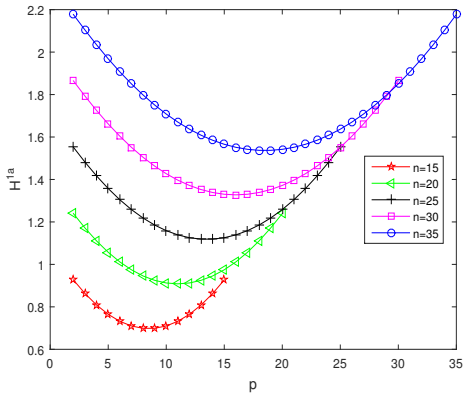

Figure 2. The influence of edge connection position p on H^{1a}.

4.2. The Influence of Edge Connection Pattern 1 & i & j on H^{1b}

When $n = 20$, through the traversal simulation of all edge connection patterns 1 & i & j, Figure 3 shows the change in H^{1b} with i, j. When $i = 2, j = 3$; $i = 2, j = n$; $i = n-1, j = n$, H^{1b} reaches the maximum value. The edge connection patterns 1 & 2 & 3, 1 & 2 & n, and 1 & $n-1$ & n have the worst network consensus.

When i is fixed, H^{1b} reaches its maximum value at $j = i+1$ and $j = n$. When $i+1 \leq j \leq (n+i+1)/2$, H^{1b} decreases as j increases. When $(n+i+1)/2 < j \leq n$, H^{1b} increases as j increases. As j can only be a positive integer, H^{1b} obtains the minimum value at $j = [(n+i+1)/2]$. The edge connection patterns 1 & i & $i+1$ and 1 & i & n have the worst network consensus, and the edge connection pattern 1 & i & $[(n+i+1)/2]$ has the best network consensus. This result is consistent with the conclusion of Conjecture 1.

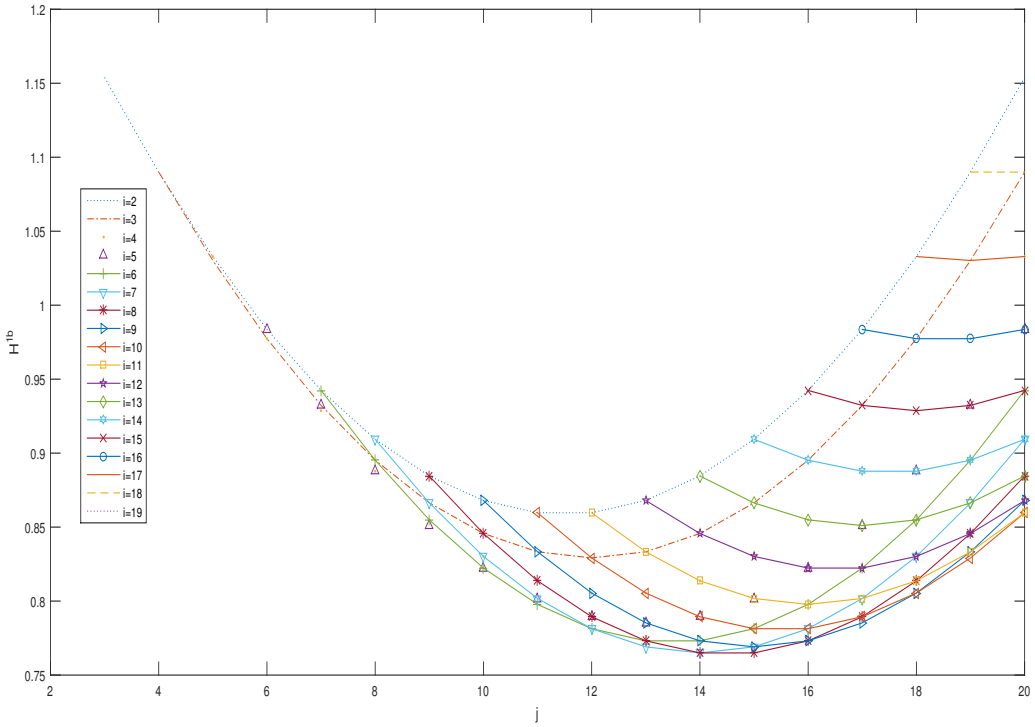

Figure 3. The influence of edge connection position j on H^{1b} when edge connection position i is fixed.

4.3. *The Influence of the Number of Single-Layer Network Nodes n on* H^{1b}

In this section, we calculate the best edge connection patterns 1 & i & j for $6 \leq n \leq 98$.

When $n = 3k + x(2 \leq k \leq 32, x = 0, 1, 2)$, Figure 4 gives an intuitive linear fitting line among i, j, and n.

As seen from Figure 4a, when $n = 3k$, the best edge connection pattern 1 & i & j is unique, and i and j are respectively distributed on the straight lines $i = k + 1$ and $j = 2k + 1$. Therefore, when $n = 3k$, the edge connection pattern 1 & $k + 1$ & $2k + 1$ has the best consensus.

As seen from Figure 4b, when $n = 3k + 1$, there are three types of best edge connection patterns; i and j are distributed on lines $i = k + 1, j = 2k + 1$, $i = k + 1, j = 2k + 2$, and $i = k + 2, j = 2k + 2$, respectively. Therefore, when $n = 3k + 1$, the edge connection patterns 1 & $k + 1$ & $2k + 1$, 1 & $k + 1$ & $2k + 2$ and 1 & $k + 2$ & $2k + 2$ have the best consensus.

As seen from Figure 4c, when $n = 3k + 2$, there are three types of best edge connection patterns; i and j are distributed on lines $i = k + 1, j = 2k + 2$, $i = k + 2, j = 2k + 2$, and $i = k + 2, j = 2k + 3$, respectively. Therefore, when $n = 3k + 2$, the edge connection patterns 1 & $k + 1$ & $2k + 2$, 1 & $k + 2$ & $2k + 2$, and 1 & $k + 2$ & $2k + 3$ have the best consensus. The above simulation results are consistent with the conclusion of Conjecture 3.

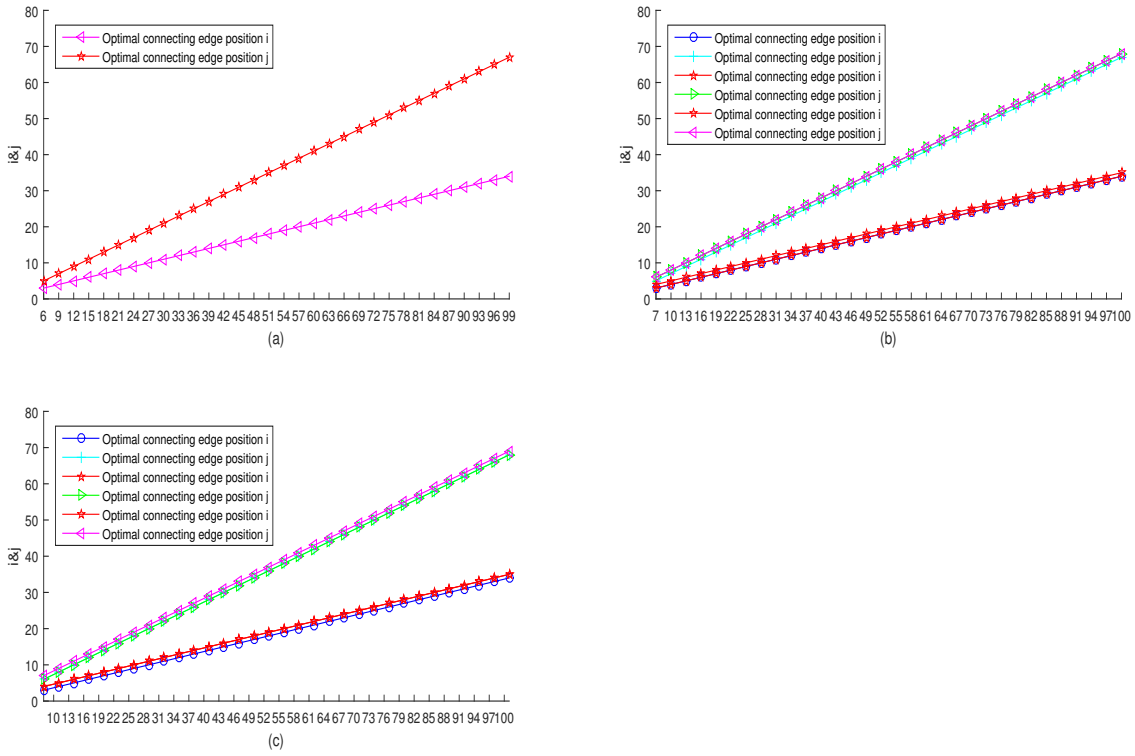

Figure 4. The relationships among the optimal edge connection positions i, j, and n. (**a**) $n = 3k$; (**b**) $n = 3k + 1$; (**c**) $n = 3k + 2$.

5. Conclusions

The research on the optimization of the interlayer connection of two-layer networks is still in the preliminary stage; the results of the theoretical method are few, and most of the results are still using the numerical method. In this study, the coherence of a Networks-a model with two linked edges between layers and a Networks-b model with three linked edges between layers were deduced using the coefficients of tridiagonal matrix characteristic polynomials and the Laplacian theorem. Furthermore, the conjectures of different edge connection patterns on the consensus of the two types of networks were obtained, which were revealed through simulation experiments. In the case of Networks-a, the best edge connection pattern is 1 & $[(n + 2)/2]$, and the worst edge connection patterns are 1 & 2 and 1 & n. In the case of Networks-b, the worst edge connection patterns are 1 & 2 & 3, 1 & 2 & n, and 1 & $n - 1$ & n. The best edge connection patterns are related to the parameter n. When $n = 3k$, the edge connection patterns are unique; when $n = 3k + 1$ and $n = 3k + 2$, there are three cases of edge connection patterns, and they are all near 1 & $k + 1$ & $2k + 1$.

The study of the effect of different interlayer connection patterns on the dynamics of two-layer networks is still at a preliminary stage, and the research results are mostly obtained using numerical methods, which is difficult to prove theoretically. This study obtained the best edge connection patterns of the networks using numerical simulations for the two-layer ring networks with two or three linked edges. However, when the number of interlayer edges is greater than or equal to four, what is the change in the best/worst edge connection patterns of the two-layer ring networks? In the case of fully connected two-layer ring networks, which edges can be reduced to obtain the best consensus? These questions are worthy of our in-depth study.

Author Contributions: Conceptualization, Z.L. and H.G.; Formal analysis, Z.S. and W.Z.; Investigation, W.Z. and H.G.; Methodology, H.G. and W.Z.; Writing—original draft, H.G. and Z.L.; Writing—review and editing, Z.S., W.Z., H.G. and Z.L.; All authors contributed equally to this work. All authors have read and agreed to the published version of the manuscript.

Funding: This research was funded by the Xinjiang Natural Science Foundation (No. 2022D01A54).

Institutional Review Board Statement: Not applicable.

Informed Consent Statement: Not applicable.

Data Availability Statement: Not applicable.

Acknowledgments: We express our sincere gratitude to the people who gave us valuable comments. This work was supported by the Xinjiang Natural Science Foundation (No. 2022D01A54).

Conflicts of Interest: The authors declare no conflict of interest.

References

1. Gelbrecht, M.; Boers, N.; Kurths, J. Variability of the low-level circulation of the South American Monsoon analysed with complex networks. *Eur. Phys. J. Spec. Top.* **2021**, *230*, 3101–3120. [CrossRef]
2. Pang, Z.; Du, T.; Zheng, C.; Li, C. Event-Triggered Cooperative Predictive Control for Networked Multi-Agent Systems with Random Delays and Packet Dropouts. *Symmetry* **2022**, *14*, 541. [CrossRef]
3. Stelzl, U.; Worm, U.; Lalowski, M.; Haenig, C.; Brembeck, F.H.; Goehler, H.; Stroedicke, M.; Zenkner, M.; Schoenherr, A.; Koeppen, S.; et al. A human protein-protein interaction network: A resource for annotating the proteome. *Cell* **2005**, *122*, 957–968. [CrossRef]
4. Liu, Y.; Xu, K.D.; Li, J.; Guo, Y.J.; Zhang, A.; Chen, Q. Millimeter-wave E-plane waveguide bandpass filters based on spoof surface plasmon polaritons. *IEEE Trans. Microw. Theory Tech.* **2022**, *70*, 4399–4409. [CrossRef]
5. Mikhalev, A.S.; Tynchenko, V.S.; Nelyub, V.A.; Lugovaya, N.M.; Baranov, V.A.; Kukartsev, V.V.; Sergienko, R.B.; Kurashkin, S.O. The Orb-Weaving Spider Algorithm for Training of Recurrent Neural Networks. *Symmetry* **2022**, *14*, 2036. [CrossRef]
6. Wu, X.; Li, Y.; Wei, J.; Zhao, J.; Feng, J.; Lu, J. Inter-layer synchronization in two-layer networks via variable substitution control. *J. Frankl. Inst.* **2020**, *357*, 2371–2387. [CrossRef]
7. He, W.; Chen, G.; Han, Q.; Du, W.; Cao, J.; Qian, F. Multiagent Systems on Multilayer Networks: Synchronization Analysis and Network Design. *IEEE Trans. Syst. Man Cybern. Syst.* **2017**, *47*, 1655–1667. [CrossRef]
8. Wu, X.; Meng, H.; Lu, J.; Jie, J.; Han, X. Analysis of the synchronizability of two-layer chain networks with two inter-layer edges. *Sci. Sin. Informationis* **2021**, *51*, 1931–1945. [CrossRef]
9. Gao, H.; Zhu, J.; Li, X.; Chen, X. Synchronizability of multi-layer-coupled star-composed networks. *Symmetry* **2021**, *13*, 2224. [CrossRef]
10. Zhu, J.; Huang, D.; Jiang, H.; Bian, J.; Yu, Z. Synchronizability of Multi-Layer Variable Coupling Windmill-Type Networks. *Mathematics* **2021**, *9*, 2721. [CrossRef]
11. Deng, Y.; Zhen, J.; Deng, G.; Zhang, Q. Eigenvalue spectrum and synchronizability of multiplex chain networks. *Phys. A Stat. Mech. Its Appl.* **2020**, *537*, 122631. [CrossRef]
12. Shang, Y. Practical consensus for heterophilous multiagent networks with constrained states. *J. Frankl. Inst.* **2022**, *359*, 10931–10948. [CrossRef]
13. Mei, G.; Wu, X.; Ning, D.; Lu, J. Finite-time stabilization of complex dynamical networks via optimal control. *Complexity* **2016**, *21*, 417–425. [CrossRef]
14. Zhang, M.; Wang, X.; Jin, L.; Song, M. Cascade phenomenon in multilayer networks with dependence groups and hierarchical structure. *Phys. A Stat. Mech. Its Appl.* **2021**, *581*, 126201. [CrossRef]
15. An, F.; Gao, X.; Guan, J.; Jiang, M.; Liu, Q. Detecting the significant nodes in two-layer flow networks: An interlayer non-failure cascading effect perspective. *Eur. Phys. J. Spec. Top.* **2019**, *228*, 2475–2490. [CrossRef]
16. Huang, D.; Yu, Z. On the Consensus Performance of Multi-Layered MASs with Various Graph Parameters-From the Perspective of Cardinalities of Vertex Sets. *Entropy* **2023**, *25*, 40. [CrossRef]
17. Shang, Y. Resilient consensus for robust multiplex networks with asymmetric confidence intervals. *IEEE Trans. Netw. Sci. Eng.* **2020**, *8*, 65–74. [CrossRef]
18. Huang, D.; Bian, J.; Jiang, H.; Yu, Z. Consensus Indices of Two Layered Multi-Star Networks: An Application of Laplacian Spectrum. *Front. Phys.* **2021**, *9*, 803941. [CrossRef]
19. Patterson, S.; Bamieh, B. Consensus and coherence in fractal networks. *IEEE Trans. Control Netw. Syst.* **2014**, *1*, 338–348. [CrossRef]
20. Sun, W.; Sun, M.; Guan, J.; Qiang, J. Robustness of coherence in noisy scale-free networks and applications to identification of influential spreaders. *IEEE Trans. Syst. Man Cybern. Syst.* **2019**, *67*, 1274–1278. [CrossRef]
21. Liu, J.; Bao, Y.; Zheng, W.; Hayat, S. Network coherence analysis on a family of nested weighted n-polygon networks. *Fractals* **2021**, *29*, 2150260. [CrossRef]
22. Chang, J.; Shi, H.; Zhu, S.; Zhao, D.; Sun, Y. Time Cost for Consensus of Stochastic Multiagent Systems with Pinning Control. *IEEE Trans. Syst. Man Cybern. Syst.* **2022**, *53*, 94–104. [CrossRef]

23. Zhang, Z.; Xu, W.; Yi, Y.; Zhang, Z. Fast Approximation of Coherence for Second-Order Noisy Consensus Networks. *IEEE Trans. Cybern.* **2022**, *52*, 677–686. [CrossRef]
24. Chen, J.; Jing, T.; Sun, W. Robustness of network coherence in asymmetric unicyclic graphs. *Int. J. Mod. Phys. B* **2021**, *35*, 2150301. [CrossRef]
25. Yi, Y.; Zhang, Z.; Patterson, S. Scale-free loopy structure is resistant to noise in consensus dynamics in complex networks. *IEEE Trans. Cybern.* **2018**, *50*, 190–200. [CrossRef]
26. Lou, Y.; Wang, L.; Chen, G. Toward stronger robustness of network controllability: A snapback network model. *IEEE Trans. Circuits Syst. I Regul. Pap.* **2018**, *65*, 2983–2991. [CrossRef]
27. Zhu, J.; Huang, D.; Gao, H.; Yu, Z.; Pei, P. Synchronizability of Multi-Layer Dual-Center Coupled Star Networks. *Front. Phys.* **2021**, *9*, 782607. [CrossRef]
28. Cao, B.; Fan, S.; Zhao, J.; Tian, S.; Zheng, Z.; Yan, Y.; Yang, P. Large-scale many-objective deployment optimization of edge servers. *IEEE Trans. Intell. Transp. Syst.* **2021**, *22*, 3841–3849. [CrossRef]
29. Lai, X.; Yang, B.; Ma, B.; Liu, M.; Yin, Z.; Yin, L.; Zheng, W. An Improved Stereo Matching Algorithm Based on Joint Similarity Measure and Adaptive Weights. *Appl. Sci.* **2023**, *13*, 514. [CrossRef]
30. Sun, L.; Hou, J.; Xing, C.; Fang, Z. A robust hammerstein-wiener model identification method for highly nonlinear systems. *Processes* **2022**, *10*, 2664. [CrossRef]
31. Shi, Y.; Xu, X.; Xi, J.; Hu, X.; Hu, D.; Xu, K. Learning to detect 3D symmetry from single-view RGB-D images with weak supervision. *IEEE Trans. Pattern Anal. Mach. Intell.* **2023**, *45*, 4882–4896. [CrossRef]
32. Wang, J.; Chen, J.; Sun, W. Network coherence of weighted duplex networks: Exact results. *Int. J. Mod. Phys. C* **2022**, *33*, 2250130. [CrossRef]
33. Jing, T.; Yang, L.; Sun, W. Exact calculations of network coherence in weighted ring-trees networks and recursive trees. *Phys. Scr.* **2021**, *96*, 085217. [CrossRef]